

For Reference

NOT TO BE TAKEN FROM THIS ROOM

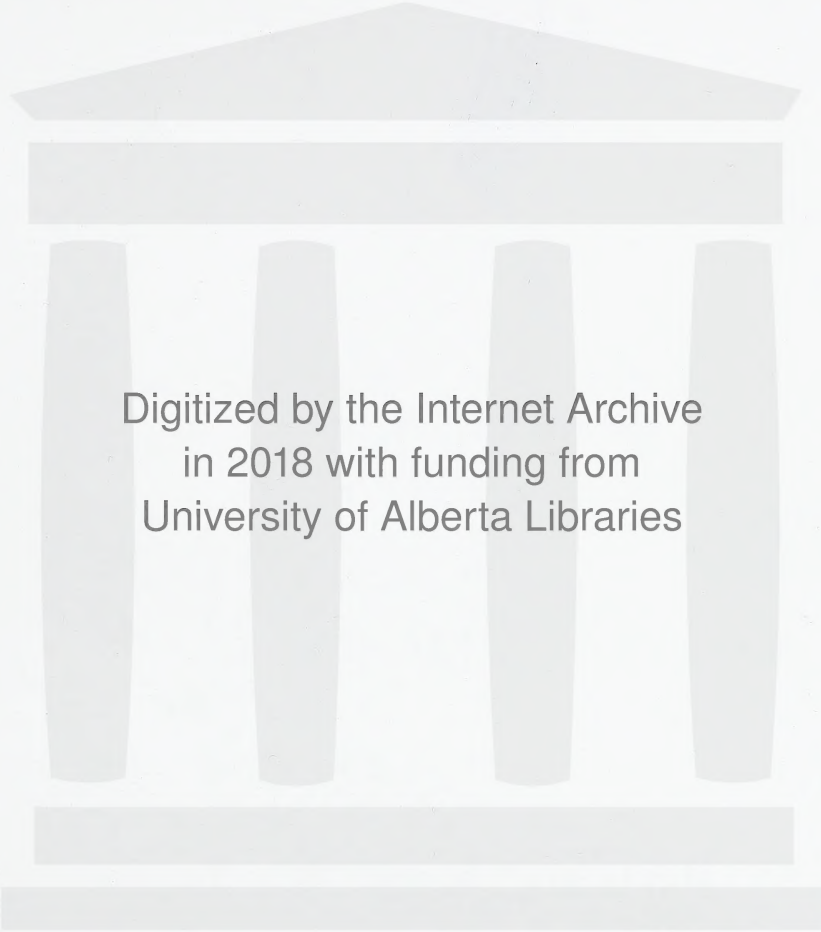
Library of the University of Alberta, Edmonton, Alberta

Smith, Archibald William
Precision determination of argon
wavelengths in the region of 3900
to 4600A.

THESIS
1952
#64

Ex LIBRIS
UNIVERSITATIS
ALBERTAENSIS





Digitized by the Internet Archive
in 2018 with funding from
University of Alberta Libraries

<https://archive.org/details/precisiondetermi00arch>

THE UNIVERSITY OF ALBERTA

"Precision Determination

of Argon Wavelengths

in the Region 3900 to 4600 Å"

A DISSERTATION

SUBMITTED TO THE SCHOOL OF GRADUATE STUDIES

IN PARTIAL FULFILMENT OF THE REQUIREMENTS FOR THE DEGREE

OF MASTER OF SCIENCE

FACULTY OF ARTS AND SCIENCE

DEPARTMENT OF PHYSICS

by

ARCHIBALD WILLIAM SMITH

Edmonton, Alberta,

August 1952.

TABLE OF CONTENTS

I	INTRODUCTION	1
II	THEORY	
	<u>1.</u> General	3
	<u>2.</u> Computation of Wavelengths	5
	<u>3.</u> Phase Change at Reflection	7
III	APPARATUS	
	<u>1.</u> General Considerations	10
	<u>2.</u> Optical System	11
	<u>3.</u> Argon Purification System	12
	<u>4.</u> Excitation	13
	<u>5.</u> The Etalon	13
	<u>6.</u> Etalon Mounting and Temperature Control	15
	<u>7.</u> Pressure Measurement	16
	<u>8.</u> Measurement of Interference Patterns	18
IV	EXPERIMENTAL PROCEDURES	
	<u>1.</u> Vacuum Exposures	21
	<u>2.</u> Air Exposures	21
V	RESULTS	
	<u>1.</u> Empirical Corrections	23
	<u>2.</u> Final Wavelength Values and Conclusions	25
	APPENDIX A	29
	APPENDIX B	30
	APPENDIX C	32
	REFERENCES	

LIST OF PLATES AND FIGURES

	following page	
Fig. 1. The Passage of Light through the Fabry-Perot Interferometer	3	
Fig. 2. Several Arrangements of Apparatus with Details of Optical System	10	
Fig. 3. The Argon Purification System	12	
Fig. 4. The Oscillator Circuit	13	
Fig. 5. Construction of the Fabry- Perot Etalon	14	
Fig. 6. The Manometer	15	
Fig. 7. Construction of Cathetometer	15	
Fig. 8. Photomultiplier Circuit	18	
Fig. 9. Apparatus for Temperature Calibration	30	
Fig. 10. Optical System for Viewing Mercury Menisci	30	
Plate I General View of Apparatus	11	
Plate II The Recording Densitometer	11	
Plate III Cathetometer and Manometer	16	
Plate IV Typical Interferometer	18	

I INTRODUCTION

In the precision determination of the wave lengths of atomic spectral lines, it is necessary that the wavelengths of certain lines be known to a high accuracy relative to the primary standard, the cadmium red line. Such lines are called secondary standards and ideally should be uniformly distributed over the entire spectral range from the vacuum ultraviolet (2000 Å) to the infrared (10,000 Å). Such a system of secondary standards is necessary in the reduction of ordinary spectrograms, which cannot be referred to the primary standard alone. At present, secondary standards known to one or two parts in 10^8 exist in the region 4200 to 7000 Å (1). They are made up of 40 lines of neon and krypton adopted by the International Astronomical Union in 1935. The lines of argon are also capable of measurement to the same precision and some measurements have already been made (2,3). The object of the research described in this thesis was to repeat some of these measurements, to improve part of the energy level scheme of argon, and to study the dispersion of air.

Precision wavelength measurements are usually made in air for convenience, and the fact that the primary standard of wavelength is defined for air at 760 mm. mercury pressure and 15°C. In the construction of energy level diagrams, the reciprocal vacuum wavelengths (wave-numbers) are required. These are computed from the values in air by using the index of refraction. At present, the value of the index is in some doubt due to the lack of agreement

among different observers (1). There are reasons (4) for believing that the index values of Barrell and Sears (5) and of Perard (6) are valid in the region 4000 Å to 10,000 Å, and some indications of a systematic error in the work of Meggers and Peters (7). In order to provide a test between the dispersion equations available, wavelengths were measured in air and in vacuum, using the averaged data of Barrell and Sears and of Perard to reduce the standard neon lines to vacuum values.

In the present work, measurements were made using a Fabry-Perot interferometer. The theory of this instrument is briefly outlined in section II, the experimental aspects in section III.

As will be seen in detail later, it is necessary to refer the measurements to at least one and preferably to two or three standard lines. The neon secondary standards were chosen because: one, it is much simpler to use several secondary standards than the primary standard alone; and two, the neon spectrum is easily produced experimentally.

II THEORY

1. General

The Fabry-Perot interferometer consists essentially of two highly reflecting, plane-parallel surfaces which are slightly transparent. In practice, these are usually obtained by using two glass or quartz discs with adjacent sides partially silvered or aluminized (reflectivity between 75 and 90%). When a ray of light strikes a surface, it is partially reflected and partially transmitted (fig. 1). The multiple reflections that occur provide a number of parallel transmitted rays with a constant phase difference. When passed through a lens, these rays combine in the focal plane to produce an interference pattern. Due to symmetry, the pattern consists of concentric bright rings.

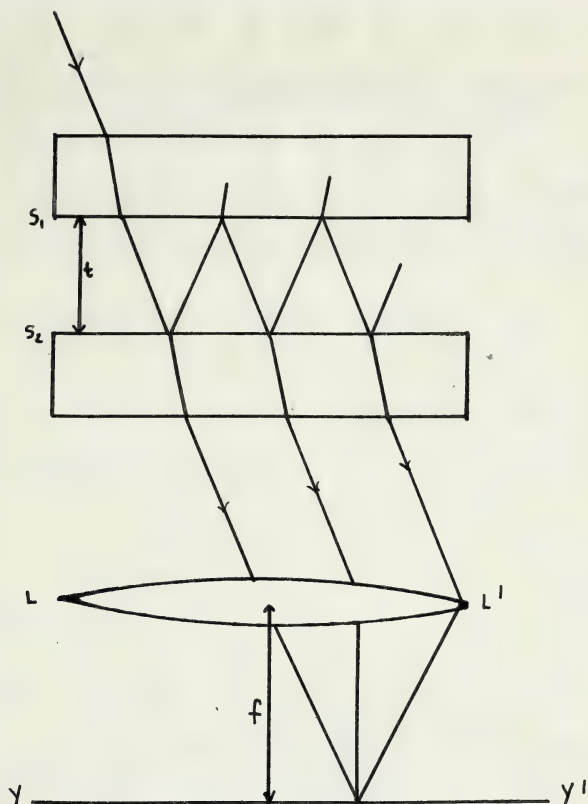
In what follows, only material necessary for the calculation of wavelengths will be considered. General treatments of the interferometer are given by Meissner (8) and by Tolansky (9).

The bright rings in the interference patterns are numbered 0, 1, 2, 3... starting at the center. The following relations may be derived (Meissner):

$$p_i = \frac{2t}{\lambda} \left(1 - \frac{D_i^2}{8f^2} \right) \quad (1)$$

$$\frac{D_K^2 - D_i^2}{K-i} = \frac{4\lambda f^2}{t} \quad (2)$$

where p_i is the order number for the i th bright ring, D_K and D_i the diameters of the K th and i th bright rings respectively, λ the wavelength, f the focal length of the lens, and t the separation of the reflecting ^{na} surfaces (etalon thickness).



S_1, S_2 Silvered or aluminized surfaces

t Etalon Thickness

LL' Lens

YY' Focal plane of lens

f Focal length of lens

Figure 1. The passage of light through the Fabry-Pérot interferometer

An order number P , which will in general be non-integral, is assigned to the center of the interference pattern. The relation

$$P = \frac{2t}{\lambda} \quad (3)$$

can easily be shown to hold (Meisner). The order at the center can also be expressed in terms of the order number of the $n+1$ ring and a fractional part ϵ as

$$P = p_n + n + \epsilon. \quad (4)$$

In order to relate ϵ to the observed fringe diameters, equations (1), (3) and (4) are combined, to give

$$\epsilon = \frac{t D_n^2}{4 \lambda f^2} - n, \quad (5)$$

which becomes, using equation (2),

$$\epsilon = \frac{D_n^2 (n-i)}{D_n^2 - D_i^2} - n \quad \text{or} \quad \epsilon = K D_n^2 - n. \quad (6)$$

It is clear from equation (2) that K is a constant for a given interference pattern.

If more than two diameters are measured, it is evident that ϵ may be found in different ways. One procedure is to use equation (6) in the form

$$K D_n^2 = n + \epsilon \quad (7)$$

and to use the method of least squares to find \bar{K} (and K if desired) by assuming that D_n^2 rather than D_n is the variable. The normal equations (see, for instance, (10)) can be written in the form

$$K \sum D_n^2 = \sum n + j \epsilon \quad (8)$$

$$K \sum n D_n^2 = \sum n^2 + \epsilon \sum n. \quad (9)$$

where all summations are from $n = 0$ to $n = j + 1$ where j is the number of values of $N D_n^2$ observed. In this particular work, five diameters were measured, in which case the expression for ϵ is

$$\epsilon = \frac{3 \sum D_n^2 - \sum n D_n^2}{\frac{1}{2} \sum n D_n^2 - \sum D_n^2} \quad (10)$$

3. Computation of Wavelengths

In order to calculate wavelengths, it is necessary to know: (a) the fractional parts ϵ for at least two standard wavelengths, (b) the fractional parts ϵ for the unknown wavelengths, (c) approximate values of the unknown wavelengths (five figures), and (d) an approximate value of the etalon thickness (± 0.005 mm.). The first step is to use items (a) and (b) to find the exact etalon thickness t . This may be done several ways (9) but the following method was used due to the availability of two Marchant computing machines. An approximate order number P for the standard lines was found using the approximate thickness and equation (3). A standard wavelength was set in the keyboard of each machine as multiplicand, while the corresponding approximate order number with the measured value of ϵ was used as a multiplier. This multiplication gives, by equation (3), an approximate value of St , which will be different for the two standards. The approximate order numbers were then varied by units (which can be done without disturbing the fractional parts) until agreement within 2 or 3 parts in 10^8 is reached for the value of St . The third standard is then used to check this value. Once an exact value of St has been found for one exposure, those following are much easier to determine as the variation in

in thickness is small if the etalon is not disturbed.

The unknown wavelength may now be found. First, approximate order numbers are calculated using item (c) above, equation (3) and the exact thickness. These order numbers are made exact by using item (b) instead of the calculated fractional part. Equation (3) is then used again with exact values of $2t$ and P to give the wavelength.

Standard wavelengths are given in air at 15°C and 760 mm. of mercury pressure. If conditions other than these are used, which is usually the case, the standard must be adjusted by using an appropriate index of refraction. The relation between density and refractive index of a gas is

$$\frac{n_1 - 1}{\rho_1} = \frac{n_2 - 1}{\rho_2}, \quad (11)$$

where n_1 and n_2 are the indices at densities ρ_1 and ρ_2 respectively. The density may be found from the temperature T and pressure P by using the ideal gas law:

$$\frac{\rho_1 T_1}{P_1} = \frac{\rho_2 T_2}{P_2}. \quad (12)$$

These equations combine to give

$$n_2 - 1 = \frac{P_2 T_1}{P_1 T_2} (n_1 - 1). \quad (13)$$

In practice, the standard wavelengths were first converted to vacuum exposures by using the relation

$$\lambda_{\text{vac.}} = n \lambda_{\text{air.}} \quad (14)$$

Then values in air corresponding to exposure conditions were calculated using the index determined from equation (7). The

actual values used for the index of refraction are given in Appendix A.

3. Phase Change at Reflection

In the process of reflection at a metallic surface, a small phase change depending upon the wavelength, is introduced between the incident and reflected rays. A small correction must be applied to the wavelength, as calculated in section 2, to eliminate the dispersive effect of the phase change. In order to do this, the wavelength must first be computed from the data of at least two different etalon thicknesses.

The phase change may be represented as an apparent change in the etalon thickness, $2\delta t$. Equation (3) becomes

$$\lambda = \frac{2t - 2\delta t}{P} \quad (15)$$

where the choice of the minus sign is arbitrary. Equation (15) now gives the exact value of the wavelength while equation (3) gives only an approximate value. Rewrite equation (3) in the form

$$\lambda_{obs.} = \frac{2t}{P}. \quad (16)$$

Subtract equation (15) from equation (16). This gives

$$\begin{aligned} \lambda_{obs.} - \lambda &= \frac{2\delta t}{P} \\ &= \frac{\lambda \delta t}{t} \end{aligned} \quad (17)$$

using an approximate value of P from equation (16). As the left hand side is small, either λ or $\lambda_{obs.}$ may be used on the right hand side. For a given wavelength, we may write

$$\lambda_{\text{obs.}} - \lambda = \frac{c}{t} \quad (18)$$

where c is a constant. We define two new quantities:

$$\Delta\lambda = \lambda_{\text{obs.}} - \overline{\lambda_{\text{obs.}}} \quad (19)$$

$$\delta\lambda = \lambda - \overline{\lambda_{\text{obs.}}} \quad (20)$$

where $\overline{\lambda_{\text{obs.}}}$ is the average of the wavelength values observed at two different etalon thicknesses. With the aid of these relations, equation (18) becomes

$$\Delta\lambda = \delta\lambda + \frac{c}{t} \quad (21)$$

By treating $\Delta\lambda$ and $\frac{1}{t}$ as variables, $\delta\lambda$ and c may be found by a least squares procedure. The normal equations (see 10) are

$$\sum \Delta\lambda = n \delta\lambda + c \sum \frac{1}{t} \quad (22)$$

$$\sum \frac{\Delta\lambda}{t} = \delta\lambda \sum \frac{1}{t^2} + c \sum \frac{1}{t^3} \quad (23)$$

where n is the number of thicknesses used. Equations (22) and (23) may be solved to give

$$\delta\lambda = - \frac{\sum \frac{1}{t} \sum \frac{\Delta\lambda}{t}}{n \sum \frac{1}{t^2} - (\sum \frac{1}{t})^2} \quad (24)$$

and

$$c = \frac{n}{\sum \frac{1}{t}} \delta\lambda. \quad (25)$$

For the particular etalon thicknesses used, these become

$$\delta\lambda = 1.271 \sum \frac{\Delta\lambda}{t} \quad (26)$$

$$c = -0.82 \delta\lambda. \quad (27)$$

In order to find the wavelengths from each etalon thickness corrected for phase change we require

$$\lambda - \lambda_{\text{obs.}} = \delta\lambda - \Delta\lambda. \quad (23)$$

The individual values of this correction for the three etalon thicknesses are:

0.5 cm. etalon.....1.64 $\delta\lambda$

1.0 cm. etalon.....0.82 $\delta\lambda$

1.5 cm. etalon.....0.55 $\delta\lambda$.

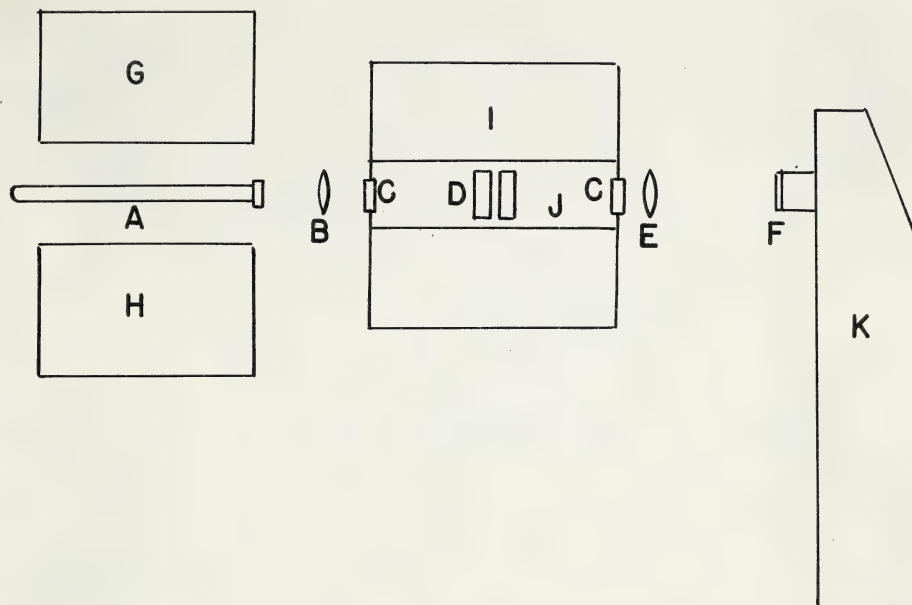
III APPARATUS

1. General Considerations

In order to use the Fabry-Perot interferometer for the measurement of wavelengths in a complex spectrum, certain auxiliary equipment is necessary. When many wavelengths fall on the interferometer, each interference pattern must be separated from the others to be measurable. This is done by "crossing" the interferometer with a spectrograph.

As the interference pattern produced depends upon the index of refraction of the gas between the plates of the interferometer, the index, and hence the density, must be kept constant during the exposure. In addition, the temperature and pressure must be measured in order to determine the wavelength at standard conditions, 760 mm. of mercury and 15 C. Constant pressure and temperature were obtained by placing the interferometer in an air-tight chamber surrounded by a thermostated water bath.

Precision required in pressure and temperature measurements: In order to measure the wavelength to eight significant figures, measurements must be correct to one part in 10^8 at 10,000 Å and five parts in 10^8 at 2000 Å. If conversions are to be made from air to vacuum values of the wavelength, the index of refraction must be known to one part in the eighth decimal place of 1.00030000 (the approximate value of the index) at 10,000 Å, and to five parts at 2000 Å. But due to the form of equation (11), the density only needs to be known to one part in 30,000 at 10,000 Å and to five parts at 2000 Å. The



- A discharge tube with quartz window
- B quartz lens, focal length 8 cm.
- C quartz windows
- D interferometer slit
- E Quartz - fluorite achromat, focal length 23 cm.
- F spectrograph slit
- G oscillator
- H argon purification system
- I water bath
- J etalon chamber
- K spectrograph

Figure 2. General arrangement of apparatus, showing details of optical system.

accuracy necessary for the temperature and pressure measurements is as follows:

At 10,000 Å, density to 1 part in 30,000 or pressure to 0.03 mm in 760 mm. and temperature to 0.01°K in 300°K .

At 2000 Å, density to 5 parts in 30,000 or pressure to 0.13 mm. in 760 mm and temperature to 0.05°K in 300°K .

As a working basis it was decided to measure the pressure to the nearest hundredth of a millimeter of mercury, and the temperature to the nearest hundredth of a degree.

2. The Optical System

The general theory of crossing the Fabry-Perot interferometer with a spectrograph is considered by Tolansky (9). The particular arrangement used is shown in figure 2.

The argon source was a discharge tube A with a quartz window used "end on". The neon source was a Geissler tube containing a capillary. Light from either source was directed onto the interferometer D with a quartz lens B, focal length 8 cm. The light passed through the vacuum-tight etalon chamber by means of quartz windows C in each end. The fringes produced by the interferometer were focussed on the slit of the spectrograph F by a quartz-fluorite achromat E, focal length 25 cm. The position of the interferometer was such that a point between the plates was focussed on the prism of the spectrograph. A Hilger E.1 Littrow spectrograph with quartz optics was used. The adjustments were the same as used in ordinary work except that a wider slit was used.

In order to center the interferometer pattern on the slit, a light

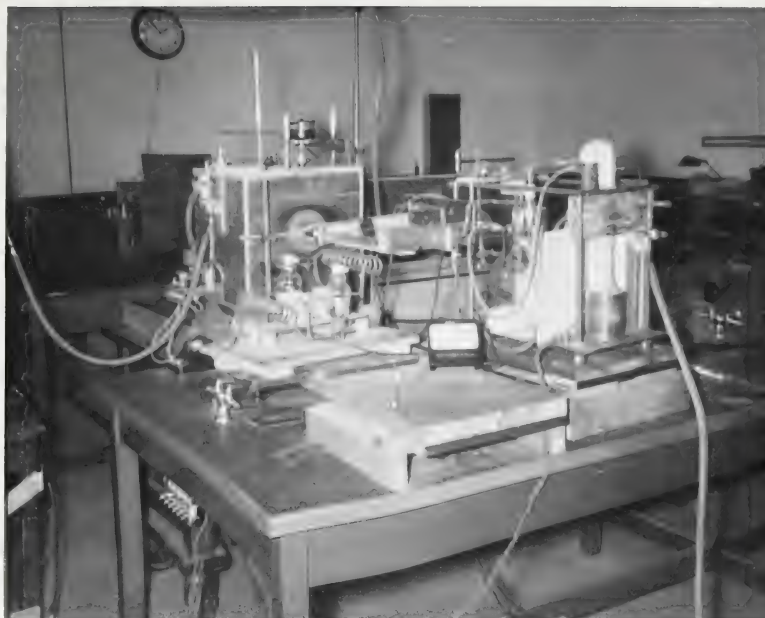


Plate I. General View of Apparatus

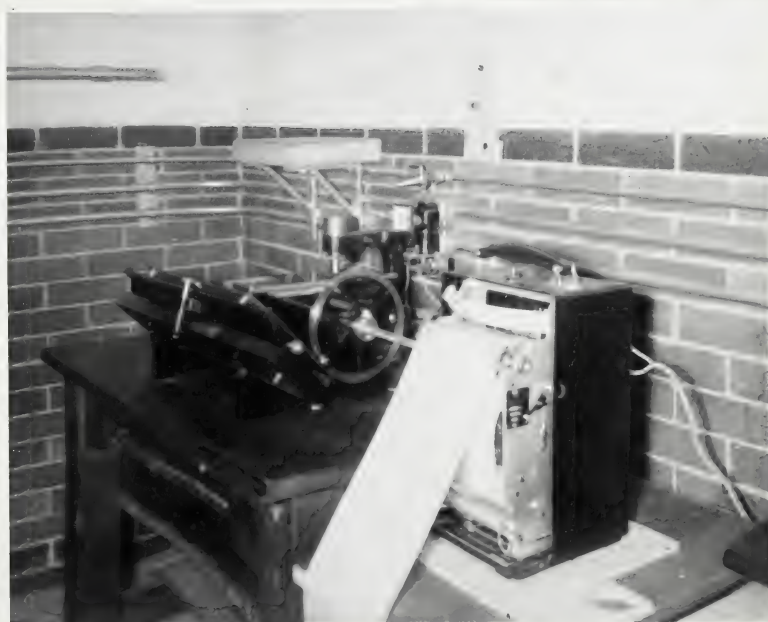


Plate II. Recording Densitometer

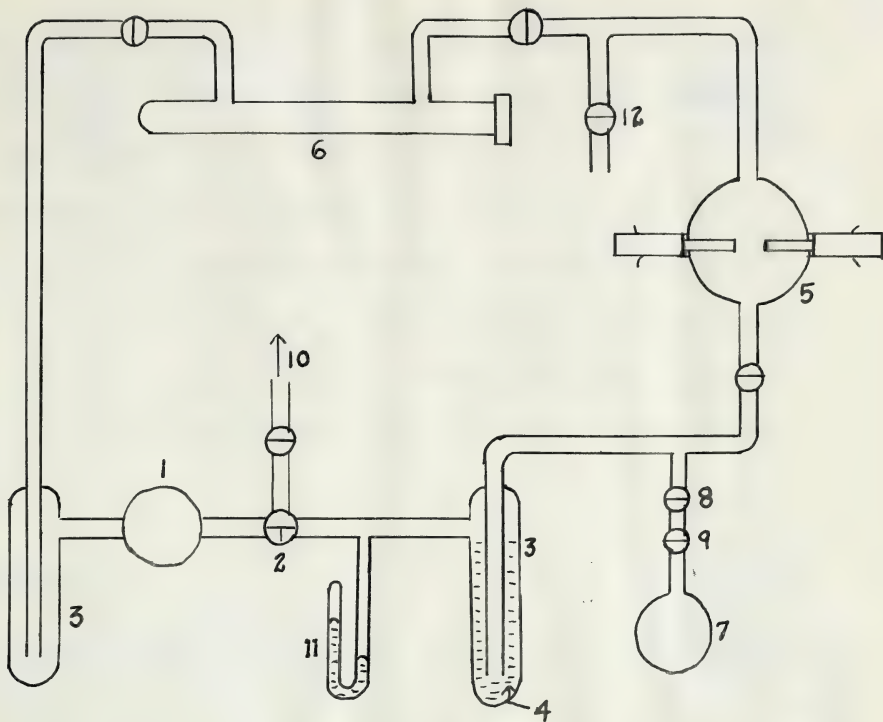
light was placed in the spectrograph. The slit image was reflected back by the interferometer and appeared beside the slit. The interferometer position was then adjusted until the slit and its image coincided. This places the interferometer mirror surfaces normal to the optic axis and the center of the pattern appears on the slit.

2. The Argon Purification System

The object of this system was to purify commercial argon. This was done by passing the argon through a charcoal trap and a discharge between magnesium electrodes (see fig. 3). Circulation was produced by a mercury diffusion pump, which was also used for the initial evacuation of the system. Traps, cooled by a solid-carbon-dioxide-acetone mixture on either side of this pump prevented mercury vapor from entering the discharge tube. One of these traps also contained charcoal which adsorbs large quantities of air at low temperature.

As the charcoal will not adsorb hydrogen appreciably, a discharge tube with magnesium electrodes was placed in the system. The magnesium reacts with the hydrogen to form a hydride. Oxides and nitrides are also formed when any air is present. The magnesium was in the form of rods which were screwed into brass plugs. These plugs were sealed to the glass discharge tube with red sealing wax. This allowed easy replacement of the magnesium. A current of 10 ma. D.C. with approximately 500 volts across the tube was used.

The source discharge tube was a piece of glass tubing 1.5 cm. in diameter and 50 cm. long with a quartz window sealed to one end.



- 1 mercury diffusion pump
- 2 three-way stopcock
- 3 traps
- 4 charcoal
- 5 discharge with magnesium electrodes
- 6 source discharge tube
- 7 flask of argon
- 8 stopcock
- 9 stopcock
- 10 to mechanical backing pump
- 11 small mercury manometer
- 12 outlet to atmosphere

Figure 3. Argon purification system

The argon was contained in a flask connected to the system through two stopcocks in series. These could be manipulated to allow small amounts of argon into the system.

The operation of such systems is considered in detail by Tolansky (9). The chief impurities appearing in the discharge tube were mercury and hydrogen. While the hydrogen was eventually eliminated, the mercury, although it became quite weak, remained. However, the mercury lines were easily identified and caused no trouble.

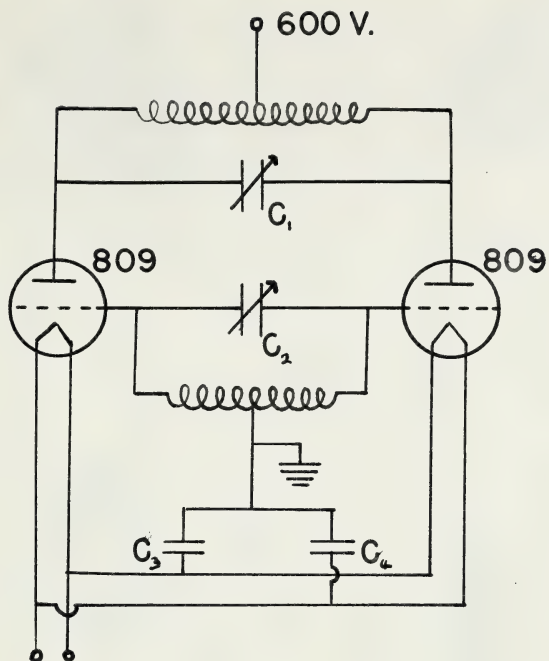
4. Excitation

A high frequency oscillator was used to excite the argon. This method gives a somewhat smaller fringe width. It is also convenient because no internal electrodes are needed in the discharge tube. The frequency was approximately 60 megacycles. Power input to the oscillator was between 50 and 100 watts.

The neon source was an ordinary Geissler tube containing a thin capillary. As the high frequency discharge would not pass through this capillary an ordinary direct current discharge was used.

5. The Etalon

The interferometer itself consisted of two quartz flats, 1.3 cm. thick and 50 cm. in diameter, aluminized on one side each to 80% reflectivity. The faces not aluminized were at a slight angle to those which were, so that secondary fringe patterns could be thrown to one



C_1, C_2 150 mmfd.
 C_3, C_4 0.5 mfd.

Figure 4. Oscillator Circuit.

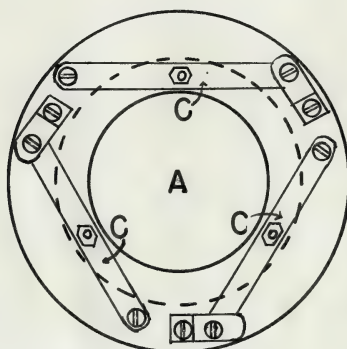
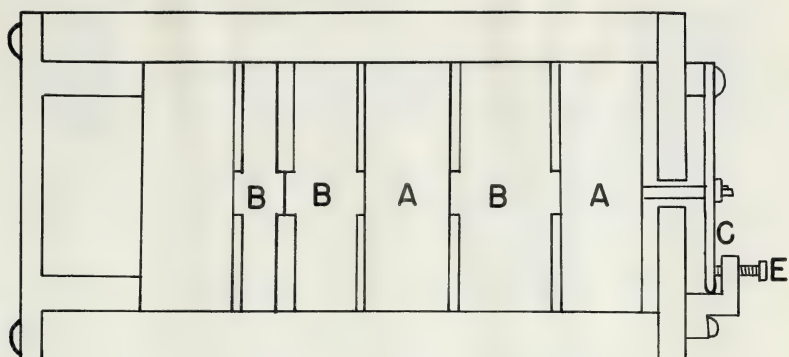
side of the main fringe pattern at the spectrograph slit (Xolansky (9))

The flats were placed in a steel sleeve together with the necessary spacer (fig. 5). Spacers not being used between the flats were placed in the sleeve so that the total length of the assembly remains constant. The spacers themselves were of invar, and had three flat projections on each side which made contact with the flats.

At one end of the sleeve, three light, adjustable springs were mounted which pressed against the flats through brass pins. These pins were placed directly above the projections on the spacers. By adjusting the tension of the springs, the aluminized surfaces of the flats could be made parallel.

Previous work (4) indicates that the temperature coefficient of the etalon is greater than that for the spacer material alone, particularly for spacers of 1.5 cm. or less. If a temperature coefficient of four times that for invar is taken, the change in separation of the flats is just one part in 10^7 for the 1.5 cm. spacer and a temperature variation of 0.02%. This indicates that some effect from temperature variations might be expected but it will be about the same size as errors of measurement.

Test for Parallelism: Fringes are observed (with the unaided eye) using the mercury green line. The eye is moved back and forth across the field. If the plates are parallel the diameters of the fringes remain constant. If a slight wedge exists, the diameters will expand as the eyes move towards the base of the wedge, due to the changing path length. The centre fringe is the most sensitive to any changes in thickness and it was used for final adjustment (4,5).



- A quartz flats
- B invar spacers
- C light springs
- D steel sleeve
- E adjusting screws

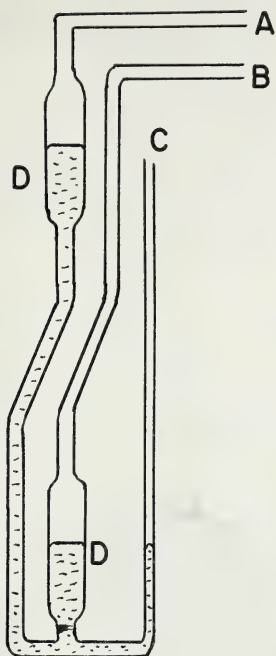
Figure 5. Construction of the Fabry - Perot Etalon

6. Etalon Mounting and Temperature Control

As shown in section 1, the temperature of the air in the etalon was required to 0.01°C . This meant that the temperature had to be kept constant to the same limit during exposures, which sometimes lasted for an hour or more. A thermostatically controlled water bath was used, temperature being monitored with a Beckmann thermometer. Its calibration is discussed in Appendix B.

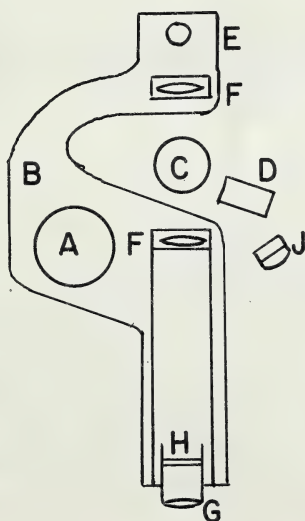
The etalon fitted snugly into a brass pipe $14\frac{1}{2}$ inches long and 3 inches inside diameter. A brass plate with a one-inch diameter quartz window was soldered on one end, while a flange one inch wide was soldered on the other. Another brass plate with a one-inch diameter quartz window was clamped against the flange, with a rubber gasket between to produce a vacuum seal. A copper tank 12 inches on a side, surrounded the central part of the brass tube. This tube, insulated with "glass wool", contained the water bath. A half-inch brass pipe soldered to the etalon chamber and fitted with rubber vacuum tubing connected the chamber to the vacuum pump and pressure measuring devices. The air used to fill the etalon chamber was dried, and had the carbon dioxide removed by means of traps containing phosphorus pentoxide and sodium hydroxide.

Temperature control was achieved by using a constant flow of cooling water through a copper coil immersed in the bath and an electric heater controlled by a mercury thermostat. The heater produced sufficient heat to overcome the effect of the cooling water. The best thermostat available opened and closed 0.02°C . apart,



- A to vacuum pump
- B to etalon chamber
- C to atmosphere
- D 2 cm. diameter tubes

Figure 6. Manometer.



- A vertical supporting rod
- B platform, swings about A
- C mercury column
- D steel scale
- E 6-volt bulb
- F lenses
- G eyepiece
- H glass scale
- J light for steel scale

Figure 7. Construction of Cathetometer

which together with the overshoot of the heating and cooling gave a range of 0.025°C . in the bath temperature. Variations of the average temperature in different parts of the bath were tested by moving the Beckmann thermometer around. These were found not exceed 0.01°C . A motor-driven stirrer was used to circulate the water around the bath.

7. Pressure Measurement

Work was done with etalon both in air and in vacuum. A MacLeod gauge (see, for instance, Hong and Korff (11)) was used to measure the residual pressure of the vacuum. When air at atmospheric pressure was used, the pressure^{was} measured with a closed mercury manometer (fig. 6). One side was kept evacuated (quality of vacuum checked with the MacLeod gauge) while the other was connected to the etalon chamber. At positions where mercury columns were to be observed, tubing of diameter 3 cm. was used, giving a very flat meniscus. The effect of mercury sticking to the glass around the meniscus was eliminated by providing an opening to the air through which the mercury could be disturbed with a small pressure change. The heights of the columns were read with a special cathetometer (fig. 7). The glass containing the mercury and cathetometer were both built around a $1\frac{1}{2}$ inch rod of cold-rolled steel. A low-power microscope was mounted by using two close-fitting sleeves on the rod. The top sleeve, to which the microscope was rigidly fixed, was free to rotate in a small angle about the rod, bearing on the lower sleeve. The contacting surfaces of the sleeves were carefully machined to insure rotation perpendicular to the rod. As a new lathe was used for this operation



Plate III. Cathetometer and manometer

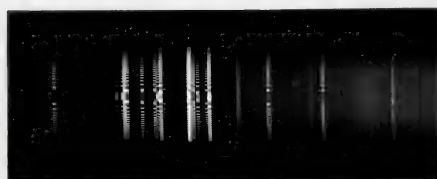


Plate IV. Typical Interferogram

it was assumed that errors from this source were considerably less than 0.01 mm. Rotation of the microscope allowed either the mercury columns or a steel scale to be observed. These were arranged so that both were at the same distance from the center of rotation and hence no refocussing was necessary. A steel scale one meter long with millimeter scale divisions was used. It was not calibrated or checked in any way. In order to get a sharp shadow of the meniscus the mercury columns were illuminated with parallel light. This was obtained by using a small 6 volt bulb and a lens. The steel scale was illuminated directly by another small 6 volt bulb. The eyepiece of the microscope contained a glass scale which was seen simultaneously with the mercury columns or steel scale. The magnification was such that 50 of these scale divisions corresponded to one millimeter on the steel scale. The position of the mercury column was noted on this scale, estimating to tenths of divisions. The microscope was then rotated to the steel scale, and the position of the nearest division on the steel scale found on the microscope scale. This gave the position to the nearest 0.002 mm.

The overall accuracy was considerably reduced by small non-uniformities in the steel rod. These flaws affected the exact position of the axis of the lower sleeve and hence it was not always parallel to the axis of the rod. In order to reduce this effect, pressure readings were made by taking a set of readings alternately at the upper and lower mercury surfaces. The average of these would then depend on the average position of the sleeve.

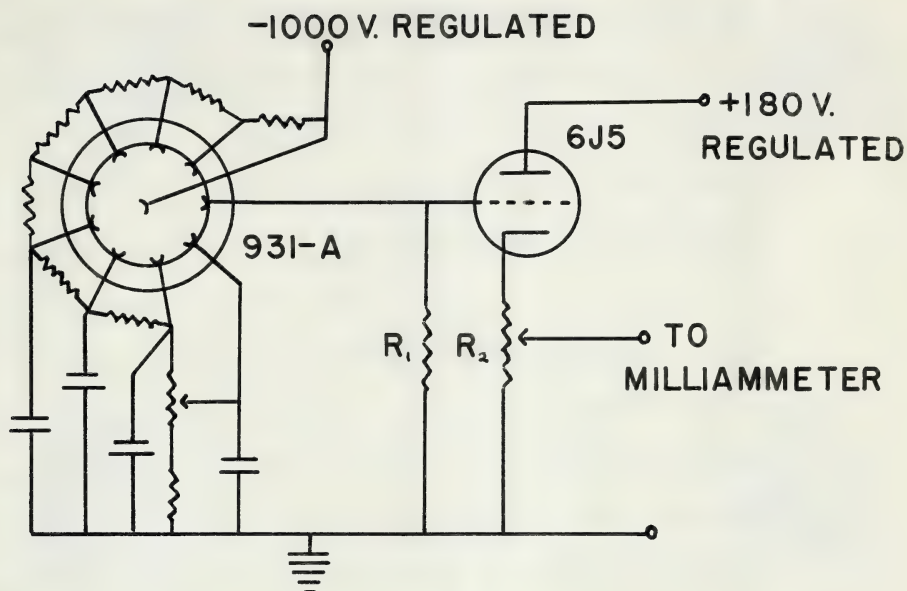
If the flaws in the rod were random, this average position would be fairly reproducible.

In obtaining final pressure readings, a correction was made for the temperature of the steel scale. A correction was also made for the temperature of the mercury, and the gravitational acceleration. These are standard at 0°C. and 980,665 cm./sec.² respectively.

8. Measurement of Interference Patterns

Measurement of the interference patterns consisted of finding the relative positions of the first five fringes on each side of the center of the pattern. The "position" of a fringe was taken as the position of greatest intensity, which was usually near the middle. The measurements were made with a visual ~~com~~^mparator or a recording densitometer. In using the comparator, a cross-bar was set on what the observer considered to be the blackest part of the fringe. This was easy to do consistently on the third, fourth and fifth fringes because they were fairly narrow. However, the first and second fringes were usually wide, and it was difficult to consistently select the densest part. This was particularly evident when two observers measured a wide fringe independently.

The densitometer gave a magnified trace of the fringe intensities on a strip of paper. The position of maximum intensity was found by bisecting the outline of the fringe near its peak. Measurement of the position of wide fringes by this method was no more difficult than measurement of thin fringes. Another advantage



R_1 470,000 ohms
 R_2 10,000 ohms
 Unmarked resistors 100,000 ohms each
 All condensers 0.01 mfd.

Figure 8. Photomultiplier Circuit.

of the densitometer was the reduction of observer fatigue. The consistency with which an observer could set on a fringe visually depended greatly on the time spent observing fringes previously. The difficulty was non-existent in the densitometer method.

While no detailed comparison of the two methods was made, it was felt that the densitometer was slightly more accurate, less subjective, and easier to use. Therefore, it was decided, eventually, to use the densitometer exclusively.

Both the comparator and densitometer were built around the same screw and carriage. No tests were made on the screw, but it was known to be of very high quality. When used as a comparator, a microscope was placed on the carriage and the plate fixed. As a densitometer, the plate was placed on the carriage while the optical system was fixed.

A conventional optical system was used in the densitometer (see, for instance, Brode (12)). It consisted essentially of two lenses, one of which focussed a spot of light from a slit source onto the photographic plate, while the other focussed the light from the plate onto a slit immediately in front of a photomultiplier tube. The source of light was a small 6 volt bulb energized by a stepdown transformer. The primary of this transformer was fed by a constant voltage transformer from the 110 volt line.

The detector was a 931-A photomultiplier, provided with 1000 volts from a regulated power supply. The photomultiplier output was fed to the grid of a 6J5 cathode follower, which

in turn fed directly to an Esterline-Angus recording milliammeter. As an average rather than a detailed outline of the fringe was desired, the cathode resistor was chosen so as to slightly overdamp the milliammeter. This meant that the milliammeter movement could not follow every detail of the fringe intensity, but produced a smooth outline. The circuit is shown in figure 10.

The external drive of the Esterline-Angus recorder was used to turn the screw. This drive made one revolution per minute, which gave the plate a speed of one mm. per minute. As a three-inch-per-minute paper speed was used, the magnification between plate and paper was about 76:1. Thus a pattern of average length, say 7 mm., was spread over 21 inches of paper and an ordinary scale could be used to measure the position of peaks relative to the paper reference lines.

IV EXPERIMENTAL PROCEDURE

1. Vacuum Exposures

The constant temperature bath was placed in operation about an hour before taking exposures to insure that the etalon had reached thermal equilibrium. The etalon chamber was evacuated during this period in order to reach a constant residual pressure. Argon exposure times varied from 10 to 90 minutes, depending on the intensity of the discharge obtainable but most exposures were of 15 to 30 minute duration. The neon exposures were made either before or after the argon and they lasted 5 to 15 minutes. It was thought that the thickness of the etalon would change very little in the few minutes between the argon and neon exposures because of the precautions taken to keep pressure and temperature constant. Separate exposures are much simpler to obtain than simultaneous because each source may be placed separately before the etalon. Eastman III-F plates were used. They are sensitive from 2000 to 6900 Å. The residual pressure was read several times during the exposures with the MacLeod gauge and the approximate temperature of the bath noted.

A total of nine plates were taken, three at each of the spacers available for the etalon.

2. Air Exposures

The procedure here was similar to that in section 1. Dry, carbon-dioxide-free air was admitted to the etalon chamber after

evacuation. An hour pause was then allowed before exposures were taken to ensure that thermal equilibrium was re-established. The temperature was read before and after the complete argon-neon exposure, readings being taken at ten second intervals over the temperature control cycle and averaging. Pressure readings were taken during the exposures, about ten for each plate. A total of nine plates were taken, three with each of the etalon spacers available.

V RESULTS

1. Empirical Corrections

When the wavelengths from the vacuum plates had been calculated as outlined in section II-3, it was found that the values obtained from the three plates taken at each etalon thickness agreed fairly well amongst themselves. However, the values from the different etalon thicknesses were not particularly consistent. No definite trend existed for all the lines as would be expected on phase change considerations only. The same situation existed for the air plates. Furthermore, when wavelengths in air were reduced to vacuum, it was found that they did not agree with the values from the vacuum plates. The differences were apparently random in nature and thus could not be explained by an error in the index of refraction.

Several effects were found which might have contributed to these inconsistencies. When the full slit length of the spectrograph was utilized, a distinct curvature was noticed in the lines. This curvature caused a slight twisting of the fringes, in opposite directions on each side of the center of the pattern.

Williams and Middleton (15), using the same type of spectrograph found that the focus was not constant along the length of spectral lines. This effect was chiefly due to astigmatism in the instrument and was not important in the formation of ordinary spectral lines. It became important when a sharp focus was desired for images at different positions along the line and was particularly noticeable when a wide slit was used. In the present work, a widening of the fringes caused by this defocussing was

observed on one side of the interference patterns. This widening probably produced a shift in the position of the densest part of the fringe and hence an error in ϵ .

A rough but simple correction for the above effects was made by assuming that the measured value of ϵ depended on the positions of the fringes relative to either end of the slit image and hence on the value of ϵ itself. This dependence of ϵ on itself is illustrated in graph I, where the deviations of etalon thicknesses (as calculated with different neon lines) from the average are shown plotted against the values of ϵ used to obtain those thicknesses. The straight-line dependence on ϵ is quite evident. If the quantities

$$\Delta(\lambda t)_i = \bar{\epsilon} - \epsilon_i \quad (30)$$

$$\Delta \epsilon_i = \bar{\epsilon} - \epsilon_i \quad (31)$$

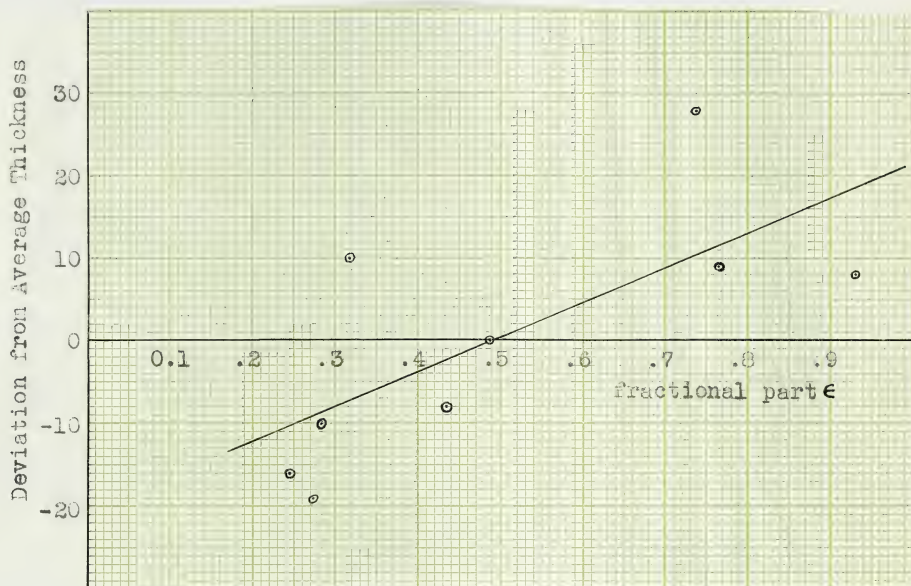
are defined, where $\bar{\epsilon}$ and $\bar{\lambda}$ are average values for neon lines and t_i and ϵ_i are individual values, the slope of the line is

$$K = \frac{\Delta(\lambda t)_i}{\Delta \epsilon_i} \quad (32)$$

This slope was found for the group of three plates at each etalon thickness, the air and vacuum plates being taken separately. A least squares procedure was used. The average value of six slopes was 43 ± 2 , which shows a good consistency.

Let ϵ' refer to the argon lines. Then the correction for ϵ' is

$$\delta \epsilon' = \frac{\Delta(\lambda t)_i}{K} \quad (33)$$



Graph I

Deviations from the Average Thickness plotted Against
the Fractional part ϵ

For plates in vacuum, etalon thickness 1.5 cm.

"Least squares" straight line is shown.



By using the relation

$$\Delta(2t) = \lambda \Delta\epsilon', \quad (34)$$

which is derived from

$$2t = (\rho + \epsilon')\lambda, \quad (35)$$

equation (32) may be written in the form

$$\delta\epsilon' = \frac{\lambda}{K} (\epsilon' - \bar{\epsilon}). \quad (36)$$

The application of the correction $\delta\epsilon'$ to ϵ' improved the agreement somewhat between the vacuum wavelengths as calculated from the plates in vacuum and in air. The results quoted in the next section include this correction.

2. Final Wavelength Values and Conclusion

The data used to compute the final vacuum wavelengths is shown in Table I. All values given include corrections for the fractional part ϵ and for the phase change at reflection. Detailed data for each plate is shown in Appendix C. Column (a) gives the first four figures of the vacuum wavelength only. Columns (b), (c) and (d) give the last four figures as calculated from plates taken in vacuum. The average value weighted according to quality of measurement, for each etalon thickness is shown and the average of these appears in column (e). Columns (f), (g) and (h) give the last four figures as calculated from plates taken in air. The average of these values appears in column (i). Column (j) gives the final vacuum wavelength, the average of columns (e) and (i).

The dispersion equation used was tested by comparing columns (e) and (i), the values of the vacuum wavelength from plates in

vacuum and in air. A statistical analysis (p. 173, ref. 10) showed that there was no significant difference between these values except in one case, the line at 4159 Å. The average of the standard deviations of all the lines was found to be 0.00043 Å (13 parts in 10^6). The difference between the dispersion equation used and that of Meggers and Peters amounts to 40 parts in 10^6 from 6000 to 4000 Å. Therefore, it may be concluded that the average dispersion of the equations of Barrell and Sears (5) and of Perard (6) is more consistent with the present data than is the dispersion of Meggers and Peters (7). It should be noted that no conclusions regarding the absolute value of the index of refraction can be drawn from this work.

The wavelengths in air at standard conditions are shown in table II, together with the values of Meggers and Humphreys and of Humphreys. It will be seen that the present values agree favorably with those of the other workers, particularly with those of Meggers and Humphreys. The values of Humphreys are somewhat higher.

Table I ARGON WAVELENGTHS IN VACUUM

a) Wavelength: first four figures	Measurement in Vacuum*				Measurement in Air*				j) Overall Average*
	b) 1.5 cm etalon		c) 1.0 cm etalon		d) 0.5 cm etalon		e) Average		
	1.5 cm etalon	1.0 cm etalon	1.5 cm etalon	1.0 cm etalon	1.5 cm etalon	1.0 cm etalon	1.5 cm etalon	1.0 cm etalon	
6418	.0765	.0882	.0764	.0770	---	---	---	---	.0770
6033	.7937	.7928	.7943	.7936	.7922	.7943	.7943	.7936	.7936
4511	.9939	.9976	.9975	.9970	.9954	.9969	.9963	.9962	.9966
4346	.3873	.3894	.3883	.3883	.3884	.3893	.3873	.3883	.3883
4336	---	---	.5559	.5559	---	---	.5546	.5546	.5553
4334	.7769	.7775	.7786	.7777	.7771	.7769	.7767	.7769	.7773
4301	.3686	.3697	.3697	.3693	.3677	.3100	.3079	.3083	.3089
4273	.3692	.3699	.3705	.3698	.3689	.3711	.3692	.3697	.3698
4267	.4846	.4861	.4832	.4853	.4840	.4865	.4838	.4848	.4851
4260	.5591	.5604	.5593	.5596	.5581	.5606	.5597	.5593	.5596
4252	---	---	.3799	.3799	---	.3812	---	.3812	.3805
4201	.8570	.8572	.8561	.8568	.8551	.8583	.8553	.8562	.8565
4199	.4995	.5000	.4994	.4996	.4980	.4990	.4976	.4982	.4989
4192	---	.2096	---	.2096	---	.2092	---	.2092	.2094
4191	.8919	.8937	.8924	.8927	---	.8933	---	.8933	.8930
4183	.0605	.0613	.0605	.0606	.0595	.0617	.0597	.0603	.0606
4165	.3521	.3525	.3524	.3523	.3515	.3522	.3503	.3513	.3518
4159	.7614	.7624	.7624	.7621	.7603	.7630	.7611	.7615	.7618
4045	.5590	.5607	.5590	.5596	.5577	.5599	.5576	.5584	.5590
3950	.0944	.0975	.0945	.0955	.0927	.0967	.0945	.0946	.0950

* Last four figures of wavelength only are given in columns b) to j).

Table II

WAVELENGTHS IN AIR AT STANDARD CONDITIONS

(a) Wavelength: first four figures	(b) Present work Ne Std.	(c) Hoggins & Humphreys Ref. (2) Ne Std. Cd Std.		(d) Humphreys Ref. (3) Kr Std.
		Ne Std.	Cd Std.	Kr Std.
6416	.3038	.315	-----	-----
6002	.1235	.124	-----	-----
4510	.7317	.7322	.7324	.7333
4345	.1669	.1666	-----	.1682
4335	.3366	.3370	.3363	.3390
4333	.5591	.5595	.5601	.5612
4300	.0993	.0995	.1000	.1011
4272	.1676	.1680	.1673	.1690
4265	.2945	.2953	.2956	.2967
4259	.3610	.3603	.3607	.3618
4251	.1839	.1842	-----	.1852
4200	.6732	.674	.6738	.6751
4198	.3162	.316	.3160	.3170
4191	.0297	-----	.0270	.0296
4190	.7122	-----	.7093	.7127
4181	.9922	.9926	.9926	.9933
4164	.1793	.1790	.1789	.1800
4136	.5939	.5936	.5936	.5906
4044	.4165	.4173	-----	.4182
3948	.9774	.977	-----	.9793

APPENDIX AThe Value of the Index of Refraction of Air

As mentioned in the introduction, the value of the index of refraction used in the present work was calculated from the averaged data of Barrell and Sears (3) and of Foward (6). The following data was obtained:

λ	$(n - 1) \times 10^7$
4000 Å	2727.0
5000 Å	2703.0
6000 Å	2709.25

The values of Kosters and Lange (12) also agree fairly well with those in the table, but as the method by which they were found is not known, they were not used. If the data is fitted with a dispersion equation of the Cauchy type, the following relation is found for dry, carbon dioxide-free air at 15°C. and 760 mm. of mercury pressure:

$$(n-1) \times 10^7 = 272.70 + \frac{1.4735}{\lambda^2} + \frac{0.02101}{\lambda^4}$$

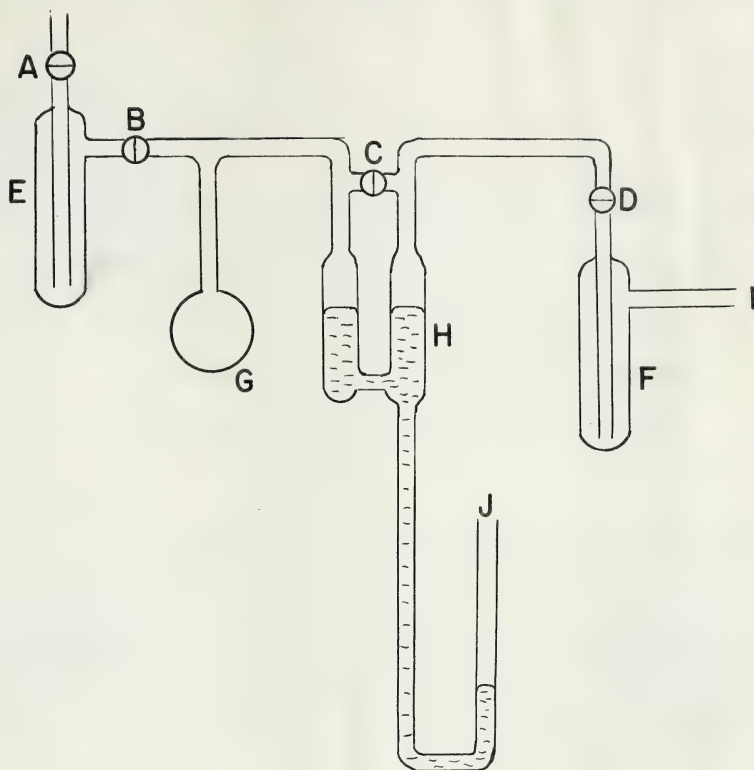
where λ is the wavelength in microns (10^{-4} cm.).

APPENDIX BCalibration of the Beckmann Thermometer

In order to calibrate the Beckmann Thermometer on the absolute scale, the saturated vapor pressure of water was used. The apparatus is indicated in figure 9.

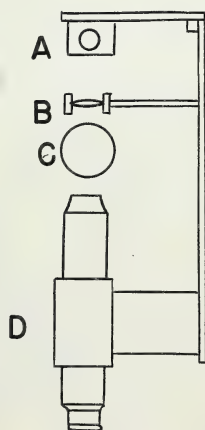
The vapor pressure was measured with two mercury columns H, which were also connected through a column of mercury to the atmosphere J. This opening allowed the mercury to be disturbed in order to eliminate sticking around the meniscus. Differences in height were found with a travelling microscope having a vernier reading to the nearest hundredth of a millimeter. In the region around 30 C., a change in temperature of the water of 0.01 C. causes a change in vapor pressure of approximately 0.01 mm., so this microscope just gave the accuracy required (see Section III-1). A sharp shadow of the mercury meniscus was obtained by illuminating it with a beam of collimated light. This light was provided by a 6-volt bulb (as a rough point source) and a lens (fig. 10).

Bulb ^G was initially placed in a solid-carbon-dioxide-acetone mixture. Water was distilled into it from trap E by evacuating with stopcocks (B), (C), and (D) open. Trap F was also placed in a dry-ice-acetone mixture to keep the water vapor out of the vacuum pump. Stopcock B was then closed and the pressure reduced to 0.01 mm. of mercury as indicated by a MacLeod gauge. At the same time, any water vapor was frozen out in either bulb G or trap F. Stopcocks C and D were then closed, and the dry-ice around bulb G replaced by a water bath in which the Beckmann thermometer



ABCD stopcocks
 EF traps
 G bulb
 H to mercury columns
 I to vacuum pump
 J to atmosphere

Figure 9. Apparatus for Temperature Calibration.



A 6-volt bulb
 B lens
 C mercury column
 D microscope

Figure 10. Optical System for Viewing Mercury Menisci.



was also immersed. The ice in bulb C melts and its vapor depresses one of the mercury columns. It should be noted that the vapor pressure of ice at the temperature of subliming dry-ice is negligible in this work.

At each temperature, twelve measurements of the difference in height of the mercury columns were made. These were averaged and corrected for any small air leaks, for the difference in height at zero pressure, and for the temperature of the mercury columns and the gravitational acceleration. These are standard at 0°C. and 980.665 cm./sec².

The observations and results are summarized in a table. Vapor pressures were converted to temperature with the aid of a table in the Handbook of Chemistry and Physics (14). A straight line was fitted to the data by the method of least squares, giving the following equation:

$$T = 0.9879 (\pm 0.0023)B + 17.4114 (\pm 0.0041)$$

where T is the temperature in degrees Centigrade, and B the reading of the Beckmann thermometer. Standard deviations of the constants are shown.

TABLE III Beckmann Thermometer Calibration Data

Beckmann Reading B	Corrected Difference in Height in mm. of Hg	Temperature in Deg. C. T
0.331	15.221	17.734
0.615	15.504	18.028
0.931	15.804	18.332
1.241	16.100	18.629
1.854	16.733	19.246

APPENDIX C

Detailed Results

The data from each of the plates in vacuum and in air are summarized in Tables IV to VI and VIII to X respectively. The fractional part ϵ for the argon lines includes the empirical correction described in Section II-1. The neon wavelengths are given in either vacuum or air at standard conditions. These were not used directly, but first adjusted to etalon conditions. This adjustment is small in the case of the vacuum plates due to the low residual pressure. In the case of the plates in air, the value of the index necessary for adjustment is given. Index values used to convert the argon wavelengths measured in air to vacuum are also given. The 'mean' of the double thickness represents a weighted average of the individual values. In some cases, two different neon exposures were measured, giving two sets of thickness values.

Tables VII and XI give the weighted average of the wavelength at each etalon thickness and the phase change correction $\delta\lambda$ calculated from these. The weights used depended on an estimate of the quality of the particular measurements. The quality was estimated by the constancy of the difference of the squares of the diameters (see Section II).

The phase change correction finally used was the average of all the values from the plates in air and vacuum. No dependence on wavelength was evident in the particular range of argon wavelengths measured (cf. Tables VII and XI). The correction thus refers to the difference in the average phase change for the neon standards and for the argon lines.

Table IV. Data from Vacuum Plates, 0.5 cm. Spacer.

Neon Wavelength at Stalon Conditions	Order Number p	Observed Fractional Part ϵ	Double Thickness 2t	Observed Fractional Part ϵ	Double Thickness 2t	Observed Fractional Part ϵ	Double Thickness 2t
5883.5248	17009	.6945	1.00073429	.6856	1.00073361	.6013	1.00073312
6031.6666	16591	.3351	73402	.3284	73376	.3213	73351
6219.0011	16091	.5550	73397	.5480	73359	.5443	73330
			mean 73409		mean 73365		mean 73333
Argon Vacuum Wavelengths*		Corrected Part ϵ	Argon Vac. Wavelength*	Corrected Part ϵ	Argon Vac. Wavelength*	Corrected Part ϵ	Argon Vac. Wavelength*
6010	15592	---	---	.4091	.0834	.3970	.0853
6033	16585	.4668	.8018	.4649	.7948	.4502	.8013
4512	22179	.3842	.0015	.3789	.0007	.3724	.0002
4346	23024	.4765	.3926	.4726	.3914	.4704	.3902
4336	23876	.6496	.5583	.6742	.5504	.6697	.5544
4334	23086	.1474	.7831	.1500	.7819	.1360	.7806
4301	23265	.7796	.3134	.7753	.3123	.7689	.3122
4273	23417	.8921	.3737	.8863	.3731	.8822	.3727
4267	23450	.1457	.4894	.1782	.4848	.1229	.4973
4260	23488	---	---	.2947	.5628	.2946	.5620
4252	23533	---	---	.4843	.3023	.4703	.3034
4201	23816	---	---	.4451	.601	.4473	.8592
4195	23829	---	---	.8160	.5922	.8205	.5001
4192	23871	---	---	.1766	.2242	---	---
4191	23873	---	---	.0688	.8041	---	---
4183	23923	.4781	.0643	.4665	.0632	.4601	.0628
4165	24025	.1706	.3572	.1742	.3548	.1567	.3511
4159	24057	.4667	.7652	.4536	.7656	.4433	.7657
4045	24736	.5593	.5622	.5790	.5622	.5757	.5615
3950	25334	.4101	.0985	.4026	.0978	.4020	.0966

** Integral part only.

* Fractional part only

Table V. Data from Vacuum Plates, 1.0 cm. Spacer.

Neon Wavelength in Vacuum	Order Number	Observed Fractional Part ϵ	Double Thickness 2t	Observed Fractional Part ϵ	Double Thickness 2t	Observed Fractional Part ϵ	Double Thickness 2t
5883.5249	34001	1.99165	2.00657003	.9775	2.00651478	.9906	2.00031555
6031.6667	33166	---	---	.9750	31532	.8808	51567
6219.0011	32167	1.6724	56996	.7848	51485	.7903	51520
			mean 57000		mean 51492		mean 51547
Argon Vacuum Wavelength	Order Number	Corrected Part ϵ	Argon Vac. Wavelength	Corrected Part ϵ	Argon Vac. Wavelength	Corrected Part ϵ	Argon Vac. Wavelength
6418	31169	1.8541	.0791	.9739	.0833	.9214	.0835
6033	33153	1.0897	.7953	.1541	.7978	.1513	.7986
6411	46337	1.9038	.9971	.6502	1.0004	.6584	1.0008
6346	46027	---	---	.0252	.7920	.0305	.7928
6336	---	---	---	---	---	---	---
6334	46150	1.6436	.7753	.3180	.7805	.3169	.7815
6301	46399	1.7240	.3093	.4119	.3121	.4027	.3128
6273	46813	1.1841	.3696	.5062	.3714	.4873	.3723
6267	46878	1.3677	.4851	.0404	.4885	.0350	.4894
6260	46954	1.5723	.5597	.2308	.5638	.2455	.5635
6252	---	---	---	---	---	---	---
6201	47616	1.5784	.8562	.2220	.8602	---	---
6199	47637	1.3123	.4982	.9467	.5029	---	---
6192	47719	---	---	.7951	.2120	.7958	.2130
6191	47723	1.7442	.8927	.3875	.8963	.3877	.8975
6183	47824	1.5148	.6602	.1536	.0640	.1534	.0650
6165	48027	---	---	.4836	.3545	.4752	.3562
6159	48392	1.3976	.7602	.0149	.7653	.0241	.7657
6045	49449	---	---	.6025	.5633	.6105	.5637
3950	50644	1.1063	.0967	.6598	.1005	.6741	.1004

* Indicates order number is increased by one.

Residual Pressure: 0.11, 0.05, and 0.05 cm. of mercury, respectively.

Table VI. Data from Vacuum Plates, 1.5 cm. Spacer.

Neon Wavelength in Vacuum	Order Number	Observed Fractional Part ϵ	Double Thickness 2t	Observed Fractional Part ϵ	Double Thickness 2t	Observed Fractional Part ϵ	Double Thickness 2t
5883.549	50998	.3185	3.00049861	.2850	3.00049659	.4862	3.00050853
6031.6667	49745	.7643	49760	.7390	49697	.9295	50861
6219.0011	44247	.2727	49832	.2446	48653	.4347	50845
			mean 49851		mean 49669		mean 50853
Argon Vacuum Wavelength	Order Number	Corrected Part ϵ	Argon Vac. Wavelength	Corrected Part ϵ	Argon Vac. Wavelength	Corrected Part ϵ	Argon Vac. Wavelength
6418	66750	.7229	.0796	.6417	.0800	.4945	.0773
6033	49728	.1995	.7970	.1648	.7978	.3797	.7951
4511	66500	.4493	.9975	.4043	.9981	.6860	.9965
4346	69034	---	---	.2541	.3285	.5205	.3888
4336	---	---	---	---	---	---	---
4334	69219	.1891	.7785	.1410	.7789	.4395	.7774
4301	69757	.7906	.3097	.7408	.3106	1.0313*	.3093
4273	70213	.8615	.3707	.8218	.3709	1.1113	.3700
4267	70310	.6936	.4854	.6380	.4866	.9241	.4858
4260	70434	.9783	.5602	.9345	.5607	1.2157	.5604
4252	---	---	---	---	---	---	---
4201	71408	.8484	.8582	---	---	1.1210	.8565
4199	71448	.9419	.5004	---	---	1.1691	.5013
4192	71513	---	---	.1746	.2088	---	---
4191	71578	.6118	.8927	.5571	.8936	---	---
4183	71729	.7186	.0620	.6653	.0629	.9880	.0604
4165	72034	.6765	.3532	.6693	.3547	.9358	.3521
4159	72131	.4833	.7628	.4455	.7628	.7326	.7620
4045	74167	.6981	.5598	---	---	.9364	.5605
3950	75960	.1523	.0955	.1013	.0960	---	---

* Indicates order number is increased by one.

Residual Pressures: 0.07, 0.10, and 0.03 mm. of mercury, respectively.

Table VII. Phase Change Correction Data for Vacuum Plates.

Vacuum wavelengths of Argon**	Weighted Average 0.5 cm. Etalon*	Weighted Average 1.0 cm. Etalon*	Weighted Average 1.5 cm. Etalon*	Overall Average* $\lambda_{obs.}$	Phase Change Correction $\delta\lambda$
6418	.0834	.0817	.0789	.0813	-0.0043
6833	.8010	.7966	.7966	.7981	42
4511	.0004	.9992	.9971	.9989	27
4346	.3912	.3910	.3885	.3902	21
4336	.5588	---	---	---	--
4334	.7415	.7791	.7781	.7796	-0.0029
4301	.3126	.3111	.3098	.3112	22
4273	.3734	.3715	.3704	.3718	25
4267	.4881	.4877	.4858	.4872	17
4260	.5622	.5620	.5603	.5615	14
4252	.3828	---	---	---	--
4201	.8590	.8588	.8582	.8587	-0.0008
4199	.5023	.5016	.5007	.5015	15
4192	---	.2112	---	---	--
4191	.8953	.8953	.8931	.8946	14
4183	.0634	.0629	.0617	.0627	12
4165	.3553	.3541	.3533	.3542	19
4159	.7653	.7640	.7626	.7640	21
4045	.5619	.5623	.5602	.5615	09
3950	.0974	.0991	.0956	.0974	06

* Fractional part of wavelength only.

** Integral part only.

Table VIII. Date from Plates in Air. 0.5 cm. Spacer.

Neon Wavelength in Air at Stand- ard Conditions	Order Number	Pressure & Temp- erature	Index* (n-1)X10 ⁸	Observed Fractional Part ϵ	Double Thickness 2t
5881.8950	17013	69.493	25024	.3238	1.00073274
6029.9971	16595	ca. Hg.	25004	.4675	73309
6217.2813	16095	18.608° C	24981	.5562	73284
					mean 73285

Argon Wavelength in Air. Integral Part Only	Argon Wavelength* in Air*	Corrected Part ϵ	Argon Wavelength**
15596	69.536	.2966	.4779
16589	ca. Hg.	.6023	.2952
22184	18.608° C	.9912	.8548
23030		.3143	2854
23082		.5289	.4558
23091		.9961	.6780
23271		.6814	.2171
23423		.8355	.2840
23456		.1210	.4034
23494		.2616	.4779
23539		---	---
23822		.4975	.7889
23835		.8770	.4307
---		---	---
---		---	---
23929		.5480	.9964
24031		.2830	.2922
24063		.5245	.7039
24742		.8278	.5270
25340		.8713	.0860

* at etalon conditions

** fractional part of wavelength only

Table VIII. Continued. Data from Plates in Air, 0.5 cm. Spacer

Pressure & Temperature	Index* (n-1) × 10 ⁸	Observed Fractional Part ϵ	Double Thickness 2t	Pressure & Temperature	Index* (n-1) × 10 ⁸	Observed Fractional Part ϵ	Double Thickness 2t
69.501 cm. Hg 18.609°C	25027 25007 2-983	.3300 .4727 .5620	1.00073305 73334 73317 mean 73316				
69.503 cm. Hg 18.609°C	24961 25007 25327 86 89 90 25402 14 16 19 22 42 44 47 47 50 54 57 25512 60	--- .6012 .9946 .3093 .5324 1.0018 .6868 .8305 .1721 .2641 --- .5007 .8795 --- --- .5440 .3836 .782 --- .8716	--- .2930 .8555 .2875 .4565 .6783 .2174 .2863 .4045 .4789 --- .7897 .4316 --- --- .9984 .2735 .7046 --- .0871				
		Corrected Part ϵ	Argon Wave-length in Air*			Corrected Part ϵ	Argon Wave-length in Air*
		--- .6012 .9880 .3117 .5299 .9746 .6809 .8316 .1379 .2611 .4797 .3088 .2890 .8743 --- --- .5432 .2832 .5747 .8285 --- 8687	--- 24958 25004 25325 84 87 87 25400 12 14 17 20 40 42 44 44 48 52 54 25509 57				

* at etalon conditions

* fractional part of wavelength only

Table IX. Data from plates in air, 1.0 cm. spacer.

Neon Wavelength in Air at Stand- ard Conditions	Order Number	Pressure & Temp- erature	Index* (n-1)x10 ⁸	Observed Fractional Part ϵ	Double Thickness 2t
5881.8950	34010	69.367 cm. Hg	2.978	.4411	2.00051306
6029.9971	33175	18.611°C	39	.1172	51318
6212.2813	32175		35	.7846	51356
					mean 51323
Argon Wavelength in Air, Integral Part only				Corrected Part ϵ	Argon Wavelength** in Air*
6416	31177	69.376	28915	---	---
6032	33163	cm. Hg	61	.4401	.2024
3410	44348	18.611°C	25281	8327	.8548
4345	46038		25379	.6595	.2009
4335	---		---	---	---
4333	46161		43	.9897	.6804
4300	46321		55	.1655	.2217
4272	46825		67	.3235	.2791
4266	46889		69	.9085	.6047
4259	46966		72	.1185	.6817
4251	47056		75	---	---
4200	47622		95	.2641	7940
4198	47649		97	.0346	.3338
4191	47731		25400	.0089	.1462
4190	47735		00	.0851	.8304
4181	47836		03	.2630	.6014
4164	48039		07	.6542	.2936
4158	48104		10	.7063	.7074
4044	49462		65	.1746	.5315
3948	50657		25512	.5006	.0911

* At etalon Conditions

** Fractional part of wavelength only

Table IX Continued. Data from Plates in Air, 1.0 cm. Spacer.

Pressure & Tem- perature	Index ^a ($n-1$) $\times 10^8$	Observed Fractional Part ^c	Double Thickness 2t	Pressure & Tem- perature	Index ^a ($n-1$) $\times 10^8$	Observed Fractional Part ^c	Double Thickness 2t
69.371 cm. Hg 18.611°C	24980 60 37	.4458 .1147 .7819	2.00051333 51306 51328 mean 51322	69.346 cm. Hg 18.613°C 69.356 cm. Hg 18.615°C	24971 51 27 74 54 31	.4422 .1130 .7896 .4420 .1111 .7816	2.00051329 51312 51408 51321 51291 mean 51345 51326
Corrected Part ^c				Corrected Part ^c / Argon Wavelength ^{a*} in Air ^a			
69.371 cm. Hg 18.611°C	24913 59 25279 25338 ---	.7317 .4167 .8418 .6739 ---	Argon Wave- length ^{a*} in Air ^a .4810 .2903 .8579 .2885 ---	69.377 cm. Hg 18.613°C	24915 61 25281 25340 ---	--- .3977 .8424 .6630 ---	--- .2829 .8379 2897 ---
	41 54 65 67 70 74 93	.9972 .1723 .3297 .9024 .1260 .4662 .2908	.6799 .2210 .2835 .4032 .4810 .3035 .7917		43 56 68 70 72 76 96	.9986 .1711 .3294 .8917 .1200 .4623 .2741	.6800 .2212 .2866 .8663 .4816 .3039 .7931
	95 98 99 25402 05 08 63 25511	.0297 .9041 .4428 273. .6526 .2084 .1745 .5441	.4343 .1448 .8506 1.0005 .2958 .7073 .5315 .6908		97 25400 00 04 07 10 65 25512	.0263 .8664 --- .2699 .6511 .2035 .1672 .5749	.4347 .1465 --- 1.0008 .2961 .7077 .5322 .0901

* at etalon conditions

** fractional part of wavelength only

Table 2. Data from Plates in Air, 1.5 cm. Spacer.

Mean Wavelength in Air at Stand- ard Conditions	Order Number ρ	Pressure at Tem- perature	Index* ($n-1$) $\times 10^3$	Observed Fractional Part ϵ	Double Thickness 2 t
5811.8930	51011	69.330	2.965	.2060	3.0008791
6029.9971	49758	cm. Hg.	45	.3306	50822
6217.2013	48259	18.611°C	22	.4559	50821
					mean 50815
Argon Wavelength in Air, Integral Part Only				Corrected Part ϵ	Argon Wavelength** in Air*
6016	46762	69.330	2.898	.5166	.5813
6032	49740		24944	.7699	.7911
5410	66517	18.611°C	25264	.4651	.8576
4345	69051		25322	.9946	.2883
4335	---		---	---	---
4333	69236		26	.9357	.6815
4300	69775		39	.6964	.2196
4272	70231		51	.9092	.2863
4266	70328		52	.7336	.4045
4259	70443		55	.5652	.4805
4251	70578		59	.3012	.3176
4200	71427		79	.1848	.7930
4198	71467		80	.3650	.6347
4181	---		---	---	---
4180	---		---	---	---
4181	71748		87	.1565	.9092
4164	72053		90	.1993	.7065
4158	72150		93	.0462	.7066
4044	74186		23448	---	---
3998	75979		96	---	---

* at etalon conditions

** fractional part of wavelength only

Table X Continued. Data from Plates in Air, 1.5 cm. Spacer.

Pressure & tem- perature	Index* (n-1)/x10 ⁸	Observed Fractional Part ε	Double Thickness 2t	Pressure & tem- perature	Index* (n-1)/x10 ⁸	Observed Fractional Part ε	Double Thickness 2t
69.588 cm. Hg	25058	.2045	3.00050496	69.310 cm. Hg	24958	.1968	3.00050752
18.610°C	25039	.3285	50518	17.609°C	15	.3166	50750
	25015	.4466	50498	69.314	58	.4422	50765
			mean 50503	cm. Hg	18	.1978	50758
69.625 cm. Hg				18.609°C	15	.3321	50843 mean
18.618°C						.4470	50795 50779
Corrected				Corrected			
Part ε				Part ε			
Argon wave- length**in Air*				Argon wave-length**			
25005	---	---	---	24892	---	---	---
51	.7737	.2845		24938	.7772	.2897	
25372	.4726	.8524		25258	.6791	.8561	
25431	.9653	.2857		25316	.9955	.2876	
---	---	---	---	---	---	---	---
34	.9423	.6767		20	.9492	.6799	
47	.7075	.2145		32	.6917	.2194	
59	.8835	.2835		44	.8954	.7865	
61	.7596	.5946		46	.7435	.4032	
63	.0897	.4741		48	.0640	.4794	
67	---	---	---	52	---	---	---
87	---	---	---	72	.2405	.7891	
89	---	---	---	74	.3198	.4334	
91	---	---	---	77	---	---	---
91	---	---	---	77	---	---	---
93	.1588	.9961		80	.1801	.9985	
99	.1923	.2916		84	.2019	.2949	
25501	.0482	.7015		87	.0514	.7050	
57	.8063	.5266		25441	.8332	.5287	
25605	---	---	---	89	.7783	.0873	

* at etalon conditions
** fractional part of wavelength only

Table XI. Phase Change Correction Data for Air Plates.

Vacuum Wavelengths of Argon**	Weighted Average 0.5 cm. Etalon*	Weighted Average 1.0 cm. Etalon*	Weighted Average 1.5 cm. Etalon*	Overall Average* $\overline{\lambda_{obs}}$	Phase Change Correction $\delta\lambda$
6418	---	---	---	---	---
6033	.8010	.7981	.7951	.7981	-0.0048
4511	.9992	.9985	.9966	.9981	20
4346	.3902	.3908 ⁹	.3896	.3902	04
4336	.5575	---	---	---	---
4334	.7796	.7785	.7783	.7788	12
4301	.3108	.3116	.3089	.3104	13
4273	.3721	.3727	.3701	.3716	14
4267	.4867	.4881	.4852	.4867	03
4260	.5626	.5622	.5593	.5614	-0.0023
4252	---	.3828	---	---	---
4201	.8582	.8599	.8563	.8581	10
4199	.5005	.5006	.4992	.5001	09
4192	---	.2108	---	---	---
4191	---	.8949	---	---	---
4183	.0626	.0633	.0607	.0622	11
4165	.3532	.3538	.3527	.3532	04
4159	.7640	.7646	.7615	.7634	14
4045	.5605	.5615	.5589	.5603	08
3950	.0974	.0983	.0939	.0965	24

*Fractional part of wavelength only.

**Integral part only.

References

- (1) Sawyer, Experimental Spectroscopy, Prentice-Hall, 1944
- (2) Meggers and Humphreys, J. Research Nat. Bur. Stand., 13, 293, 1934
- (3) Humphreys, J. Research Nat. Bur. Stand., 20, 17, 1938
- (4) Newbound, J. Opt. Soc. Am., 30, 835, 1949
- (5) Barrell and Sears, Trans. Roy. Soc. (London), 238A, 1, 1939
- (6) Perard, Trav. Bur. Int. Poids Mes., 19, 1934
- (7) Meggers and Peters, Nat. Bur. Stand. Sci. Pap., 327, 697, 1918
- (8) Meissner, J. Opt. Soc. Am., 31, 405, 1941
- (9) Tolansky, High Resolution Spectroscopy, Methuen, 1947
- (10) Kenney and Keeping, Mathematics of Statistics, 2nd edition,
Van Nostrand, 1951
- (11) Hoag and Korff, Electron and Nuclear Physics, 3rd edition,
Van Nostrand, 1948
- (12) Brode, Chemical Spectroscopy, Wiley, 3rd edition, 1943
- (13) Kosters and Lampe, Physik. Zeits., 35, 223, 1934
- (14) Handbook of Chemistry and Physics, 32nd edition, Chemical
Rubber Publishing Co.
- (15) Williams and Middleton, Proc. Roy. Soc., 172A, 159, 1939

Acknowledgements

The candidate takes pleasure in thanking Dr. K. B. Newbound for his constant attention while directing the work. Thanks are also due Dr. Newbound for performing many of the tedious numerical calculations involved.

Mr. F. Gleave gave valuable assistance with the apparatus.

Appreciation is extended to other members of the Department of Physics and to fellow students for their encouragement and assistance during the course of the work.

The work was supported by grants from the National Research Council.

B29766